scientific reports

Check for updates

OPEN

Relationships between capnogram parameters by mainstream and sidestream techniques at different breathing frequencies

József Tolnai[1], Ferenc Rárosi[1], Ibolya Tóth[1], Barna Babik[2], Zoltán Novák[3], Ferenc Peták[1,4]✉ & Gergely H. Fodor[1,4]

Capnography, routinely used in operating rooms and intensive care units, reveals essential information on lung ventilation and ventilation–perfusion matching. Mainstream capnography directly measures CO_2 in the breathing circuit for accurate analysis and is considered a reference technique. Sidestream capnography, however, analyzes gas away from the patient leading to potentially less accurate measures. While these methodological differences impact the capnogram indices in mechanically ventilated patients, such assessments during spontaneous breathing are essentially lacking. Accordingly, we aimed to compare mainstream and sidestream capnography in spontaneously breathing subjects, focusing on differences in capnogram shape and dead space indices at various respiratory rates. Simultaneous mainstream and sidestream time and volumetric capnography were performed on spontaneously breathing adults (n = 35). Measurements were performed during controlled low (10/min), medium (12/min), and high (20/min) breathing rates as a challenge. Correlation and Bland–Altman analyses were used to assess trends and agreements between time and volumetric capnography indices obtained by the mainstream and sidestream techniques, including end-tidal CO_2 (ETCO$_2$), shape factors reflecting the slopes of phases 2 and 3, and anatomical and physiological dead space fractions. ETCO$_2$ and physiological dead space measured by mainstream and sidestream techniques showed excellent correlations (r > 0.90, p < 0.001 for all breathing rates) and agreements. While strong correlations and moderate agreements were evidenced in the parameters reflecting the late phase of expiration (phase 3 slope and exhaled CO_2 volume), these relationships were weaker for indices related to the early phase of expiration (phase 2 slope, anatomical dead space). Changing breathing frequency caused significant alterations in all capnography parameters, which were detectable by both mainstream and sidestream techniques. Sidestream capnography cannot substitute the more accurate mainstream technique for measuring the absolute values of shape factors and ventilation dead space fractions. However, sidestream capnography is also able to detect and track changes in uneven alveolar emptying, ventilation–perfusion matching and ventilation dead space fraction in spontaneously breathing subjects.

Keywords Spontaneous breathing, Main- and sidestream capnography, Time and volumetric domains, Dead spaces

Abbreviations

ANOVA	Analyses of variance
ANCOVA	Analysis of covariance
CO_2	Carbon dioxide
CONSORT	Consolidated standards of reporting trials
ETCO$_2$	End-tidal carbon dioxide concentration

[1]Department of Medical Physics and Informatics, University of Szeged, 9 Korányi Fasor, Szeged 6720, Hungary. [2]Department of Anaesthesiology and Intensive Therapy, University of Szeged, 6 Semmelweis Str., Szeged 6725, Hungary. [3]Department of Pediatrics and Pedriatic Health Center, University of Szeged, 14-15 Korányi Fasor, Szeged 6720, Hungary. [4]Ferenc Peták and Gergely H. Fodor have contributed equally to this work. ✉email: petak.ferenc@med.u-szeged.hu

$PACO_{2,MS}$	Mean alveolar partial pressure of CO_2 based on the mainstream technique
$PACO_{2,SS}$	Mean alveolar partial pressure of CO_2 based on the sidestream technique
$P\bar{E}CO_{2,MS}$	Mixed expired CO_2 partial pressure based on the mainstream technique
$P\bar{E}CO_{2,SS}$	Mixed expired CO_2 partial pressure based on the sidestream technique
$S2_T$	Phase 2 slope in the time domain
$S2_{T,MS}$	Mainstream phase 2 slope in the time domain
$S2_{T,SS}$	Sidestream phase 2 slope in the time domain
$S2_V$	Phase 2 slope in the volumetric domain
$S2_{V,MS}$	Mainstream phase 2 slope in the volumetric domain
$S2_{V,SS}$	Sidestream phase 2 slope in the volumetric domain
$S3_T$	Phase 3 slope in the time domain
$S3_{T,MS}$	Mainstream phase 3 slope in the time domain
$S3_{T,SS}$	Sidestream phase 3 slope in the time domain
$S3_V$	Phase 3 slope in the volumetric domain
$S3_{V,MS}$	Mainstream phase 3 slope in the volumetric domain
$S3_{V,SS}$	Sidestream phase 3 slope in the volumetric domain
$Sn2_T$	Normalized phase 2 slope of the time capnogram
$Sn2_V$	Normalized phase 2 slope of the volumetric capnogram
$Sn3_T$	Normalized phase 3 slope of the time capnogram
$Sn3_V$	Normalized phase 3 slope of the volumetric capnogram
SD	Standard deviation
VDB_{MS}	Bohr's physiological dead space based on the mainstream technique
VDB_{SS}	Bohr's physiological dead space based on the sidestream technique
VDF_{MS}	Fowler's anatomic dead space based on the mainstream technique
VDF_{SS}	Fowler's anatomic dead space based on the sidestream technique
VnDB	Bohr's physiological dead space fraction
VnDF	Fowler's anatomic dead space fraction
VT	Tidal volume

Capnography is a real-time, effort-independent respiratory monitoring modality that represents the breath-to-breath dynamics of exhaled carbon dioxide (CO_2) concentration[1–5]. The shape of the capnogram curve can reveal essential information about lung ventilation, ventilation-perfusion matching, and metabolic status[5,6]. It is routinely used in operating rooms and intensive care units. However, capnography is now also emerging in other medical specialties as a monitoring and diagnostic tool, such as in pulmonology[7–9], sleep medicine[10–12], and pediatrics[13–15]. Its wider application is further facilitated by its ability to quantify ventilation dead space parameters when combined with measurements of expired volume[5,16]. While capnography has become a mandatory monitoring tool in ventilated patients, its potential to assess cardiopulmonary status has also been recognized in spontaneously breathing subjects.

Based on the measurement site of the CO_2 concentration, mainstream and sidestream capnography are available. Mainstream capnography employs an infrared sensor directly in the breathing circuit, offering precise CO_2 analysis of the entire volume of expired gas near the patient. Conversely, sidestream capnography analyzes the expired gas distal to the patient by sampling a portion of the expired gas. However, the accuracy of sidestream capnography is limited by the smaller volume of gas analyzed, its slower response time[17,18], and the risk of gas mixing[3,19], which may contribute to the dynamic distortion of the CO_2 curve, especially at high respiratory rates[19,20]. Consequently, significant differences have been observed in the capnogram shape factors and dead space parameters between mainstream and sidestream techniques in mechanically ventilated patients[20]. Nonetheless, fundamental differences in pressure conditions exist between mechanical ventilation and spontaneous breathing, leading to a gap in knowledge regarding how spontaneous breathing influences the relationship between the two capnography techniques.

Therefore, our objective was to compare shape factor and dead space parameters measured by mainstream and sidestream capnography in spontaneously breathing subjects. To uncover potential differences stemming from the distinct dynamic responses of the two methods, we introduced varying respiratory rates as a challenge.

Materials and methods
Participants
The study protocol was approved by the Regional and Institutional Review Board of Human Investigations of the University of Szeged, Hungary (No. 186/2020; address: 6720 Szeged, Dugonics tér 13. Hungary, 25 January 2021), and the participants gave their written informed consent to take part in the study. The study was performed in accordance with the ethical standards laid down in the 1964 Declaration of Helsinki and its later amendments. The study followed the applicable CONSORT guidelines, and the patient flow chart is shown in Fig. 1. Selection criteria were: informed consent, age above 18 years, and ability to collaborate. Exclusion criteria were not set.

Thirty-six volunteers were included in the study between December 2021 and June 2022. The demographics of the subjects are demonstrated in Table 1. Regarding the underlying clinical conditions of the subjects, 3 subjects had treated hypertension, 2 subjects had type 2 diabetes, 6 subjects had pollen allergy (out of season for all of them), 2 subjects had asthma under medical control and 2 subjects were smokers. One healthy subject was excluded from the analyzes due to inappropriate cooperation.
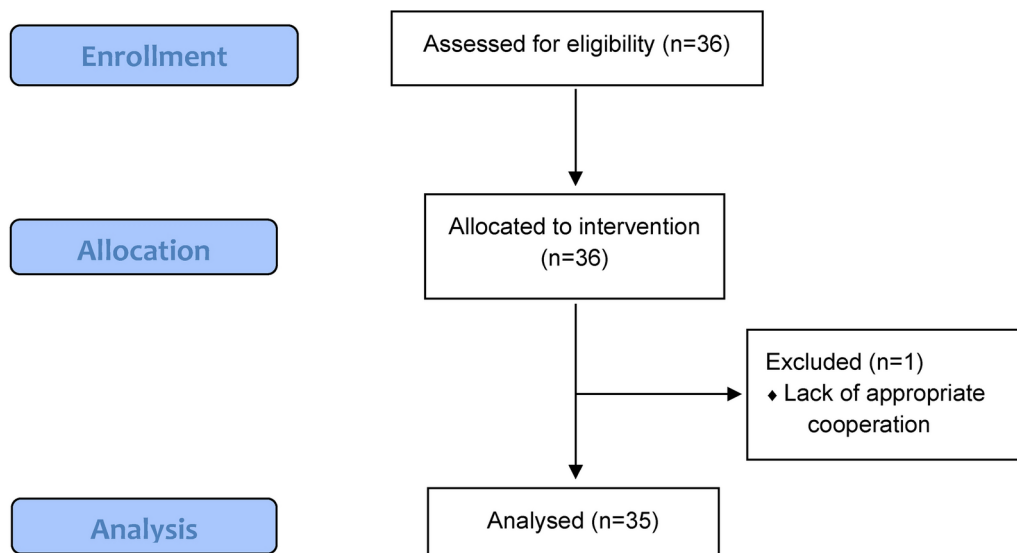
Fig. 1. Patient Flow Chart: A total of 36 participants were enrolled in the study, with selection criteria including informed consent, being over 18 years of age, and the ability to cooperate. All volunteers were eligible for the intervention; however, one patient was excluded due to a lack of appropriate cooperation.

Female/Male (n)	21/14
Age (years)	44.1 ± 13.8
Height (cm)	172 ± 9
Weight (kg)	73.7 ± 12.7
Body mass index	24.8 ± 3.4
Current smokers (n)	2
Hypertension (n)	3
Type 2 diabetes	2
History of asthma (n)	2
Allergy	6
Former COVID-19 infection (n)	4

Table 1. Patient characteristics expressed as number of patients (n) or mean ± SD.

Recording and analyses of capnograms

The measurement set-up is designed to provide simultaneous sampling of the mainstream (Novametrix, Capnogard®, Andover, MA, USA) and sidestream (Datex Oscar II™, Datex-Ohmeda, Helsinki, Finland) capnograms and the central airflow by a screen pneumotachograph (Piston Ltd, Budapest, Hungary). The CO_2 and ventilation flow signals were digitized at a sampling rate of 256 Hz and analyzed using custom-developed software.

For each expiratory cycle, the volumetric capnogram curves were determined separately from the mainstream and sidestream CO_2 partial pressure recordings, and from the volume signals obtained by integrating the corresponding flow data. The sidestream time capnogram recordings were offset by -0.46 s relative to the flow signals to adjust for the transport delay caused by the gas being drawn into the analyzer. This time gap was calibrated by inspecting the difference between the main and sidestream capnogram signals as the carbon dioxide concentration gradually changed.

The evaluation of the shape indices for both capnograph (main- and sidestream) curves and in both domains (time and volume) was based on the concepts described earlier[21,22]. Briefly, the second phase slopes of the mainstream and sidestream capnograms, which reflect the combined emptying of the airway-alveolar compartments, were calculated from the slope obtained at the inflection point in both the time ($S2_{T,MS}$ and $S2_{T,SS}$) and volume ($S2_{V,MS}$ and $S2_{V,SS}$) domains. Phase 3 slopes of the time and volumetric capnograms, reflecting the dynamics of the alveolar space emptying, determined by main- ($S3_{T,MS}$ and $S3_{V,MS}$) and sidestream capnography ($S3_{T,SS}$ and $S3_{V,SS}$) were defined by a linear regression fitted to the middle third of phase 3. Since the slopes of the capnogram curves are affected by the end-tidal CO_2 concentration ($ETCO_2$), these variables were also expressed as normalized values to the respective $ETCO_2$ levels; these normalized phase 2 and phase 3 slopes are denoted by Sn2 and Sn3 prefixes, respectively.

The generated volumetric capnogram curves also allowed the calculation of dead spaces for both measurement techniques. The Fowler dead space, representing the anatomical dead space, was defined as the volume exhaled up to the inflection point of phase 2 from the main- and sidestream (VDF_{MS} and VDF_{SS}) capnograms[23]. The physiological dead space according to Bohr (VDB_{MS} and VDB_{SS}) was calculated from the main- and sidestream capnograms as[24]:

$$VDB_{MS}/V_T = \left(PACO_{2,MS} - P\overline{E}CO_{2,MS}\right)/PACO_{2,MS}$$

$$VDB_{SS}/V_T = \left(PACO_{2,SS} - P\overline{E}CO_{2,SS}\right)/PACO_{2,SS}$$

where $PACO_{2,MS}$ and $PACO_{2,SS}$ are the mean alveolar partial pressure of CO_2, obtained by taking the value at the midpoint of phase 3 in the main- and sidestream volumetric capnograms. $P\overline{E}CO_{2,MS}$ and $P\overline{E}CO_{2,SS}$ are the mixed expired CO_2 partial pressure values, determined in each expiratory cycle by dividing the integrated MS and SS volumetric capnogram curves by the current expired gas volume (V_T). The Fowler and Bohr dead space fractions (VnDF, VnDB) were obtained by dividing the corresponding dead space volumes by V_T. Minute ventilation (MV) was calculated as the product of respiratory rate and the current expired V_T.

Study protocol

Participants were instructed to breathe through the mouth and wear a noseclip. The experimental setup included a mouthpiece, a bacterial filter, the sampling cuvette of the mainstream capnograph, the screen pneumotachograph, and the connection of the sidestream capnograph's sampling port. During the measurement phase, participants were instructed to synchronize their breathing with a metronome app (Metronome-reloaded, by Chris and Uwe, downloaded from Apple App Store) for 90 s, while volumetric capnography data with both devices was recorded. Following this, participants were instructed to remove the nose clip and breathe spontaneously for 3 min without any specific guidance before the start of another recording epoch.

This entire procedure was repeated at three different breathing rates: first at 12 breaths per minute (medium rate), then at 9 breaths per minute (low rate), and finally at 20 breaths per minute (high rate).

Statistical analysis

Sample size estimation was performed based on previous capnography data obtained from mechanically ventilated patients[20] using the differences between $S3_{T,MS}$ and $S3_{T,SS}$ to allow for Bland–Altman analyses using a level of significance (α, type I error) of 0.05 and a power (1-β) of 0.9 (type II error of 0.1). The estimation resulted in a need for a minimum of 34 subjects. The estimations were carried out using the software MedCalc (version 20.218, MedCalc Software Ltd, Ostend, Belgium; https://www.medcalc.org).

Continuous variables are described as mean and standard deviation (SD), if normally distributed, or median and minimum–maximum, if not normally distributed. Two-way repeated measures analyses of variance (ANOVA) were used for comparisons between mean values of capnography indices using capnography device (mainstream or sidestream) and breathing frequency (medium, low, or high) as factors of comparison. Pairwise comparisons were performed by using Holm-Sidak post hoc analyses. Correlations of the indices between the two devices were examined by applying a Pearson correlation test. Correlation coefficients for the same parameter under different breathing frequencies were compared by applying Fisher z-transformation on all correlation coefficients, then performing pairwise comparisons z-tests using asymptotic normality. Bonferroni correction was applied to the P values to correct for multiple comparisons. The agreement of various capnography indices between mainstream and sidestream capnography was assessed by using Bland–Altman plots[25]. Effects of breathing frequency on the agreement and its proportional error were assessed using repeated measures mixed analyses of covariance (ANCOVA) using breathing frequency as a factor and average value obtained from mainstream and sidestream capnography as a covariate of comparison with least significant difference (LSD) adjustments used for pairwise post hoc analyses.

The statistical tests were performed with SigmaPlot (version 13, Systat Software, Inc., Chicago, IL, United States) and IBM SPSS Statistics (version 29.0.0.0, IBM Corp., Armonk, NY, USA). Statistical analyses were conducted with a significance level of $p < 0.05$, and all reported p-values are two-sided.

Results

Figure S1 in the online data supplement displays time and volumetric capnography curves, measured using both main- and sidestream techniques, in a representative patient at low, medium, and high breathing rates.

Table 2 displays ventilation parameters and capnography indices across different breathing rates, using both main- and sidestream techniques. An increase in breathing frequency resulted in a decrease in V_T and an increase in MV, leading to lower $ETCO_2$ values. However, $ETCO_2$ values were consistent across breathing rates, regardless of the measurement technique. In contrast, capnography shape factors and dead space parameters measured by main- and sidestream methods showed significant differences ($p < 0.001$), except for VDF at low and medium breathing rates. Notably, there were significant increases in $S2_T$ ($p < 0.001$), $S2_V$ ($p < 0.001$), $S3_T$ ($p < 0.001$), and $S3_V$ ($p < 0.005$) with higher breathing frequencies, while VDB remained unaffected by changes in breathing rate.

Figure 2 illustrates normalized shape factors and ventilation dead space parameters measured with both main- and sidestream capnography at varying breathing frequencies. All normalized shape factors ($p < 0.001$) and VnDF ($p < 0.05$) showed significant differences between measurements from main- and sidestream capnograms, except for VnDB, which was unaffected by the measurement technique. An increase in breathing frequency significantly raised $Sn2_T$ ($p < 0.001$), $Sn3_T$ ($p < 0.001$), $Sn3_V$ ($p < 0.001$), VnDF ($p < 0.01$), and VnDB ($p < 0.01$), whereas $Sn2_V$ significantly decreased at higher breathing frequencies ($p < 0.01$).

	Low		Medium		High	
	Mainstream	**Sidestream**	**Mainstream**	**Sidestream**	**Mainstream**	**Sidestream**
f (bpm)	10		12		20	
V_T (l)	$1.1 \pm 0.5^*$		$1.0 \pm 0.3^\#$		$0.8 \pm 0.3^{*\#}$	
MV (l/min)	$11.3 \pm 3.9^*$		$13.5 \pm 3.5^\#$		$15.3 \pm 5.9^{*\#}$	
$ETCO_2$ (mmHg)	$33.3 \pm 4.8^*$	$33.4 \pm 5.2^*$	34.7 ± 4.0	35.1 ± 4.8	$29.4 \pm 4.6^{*\#}$	$28.3 \pm 5.0^{*\#}$
$S2_T$ (mmHg/s)	$118 \pm 26^*$	$101 \pm 15^{\$*}$	$138 \pm 31^\#$	$114 \pm 18^{\$\#}$	$147 \pm 31^*$	$105 \pm 16^{\$*\#}$
$S2_V$ (mmHg/ml)	221 ± 59	$180 \pm 58^\$$	233 ± 56	$184 \pm 57^\$$	$191 \pm 54^{*\#}$	$104 \pm 34^{\$*\#}$
$S3_T$ (mmHg/s)	$1.8 \pm 0.6^*$	$2.2 \pm 0.7^{\$*}$	$2.3 \pm 0.8^*$	$3.0 \pm 0.9^{\$\#}$	$3.3 \pm 0.9^{*\#}$	$4.6 \pm 1.2^{\$*\#}$
$S3_V$ (mmHg/ml)	5.5 ± 1.8	$7.7 \pm 4.5^\$$	5.9 ± 2.6	$9.6 \pm 5.6^\$$	$8.5 \pm 7.5^{*\#}$	$11.6 \pm 6.0^{\$*\#}$
VDF (ml)	119 ± 49	$98 \pm 26^\$$	130 ± 37	$106 \pm 25^\$$	$166 \pm 44^{*\#}$	$112 \pm 35^{\$\#}$
VDB (ml)	189 ± 54	193 ± 57	197 ± 48	194 ± 42	204 ± 60	$176 \pm 29^\$$
VCO_2 (ml)	$40.3 \pm 13.6^*$	$40.3 \pm 13.8^*$	$38.4 \pm 12.9^\#$	$37.3 \pm 12.0^\#$	$20.8 \pm 8.5^{*\#}$	$19.1 \pm 8.1^{\$*\#}$

Table 2. Ventilation parameters and capnography indices obtained at low, medium and high breathing frequencies in spontaneously breathing subjects (n = 35). f: Breathing frequency, V_T: Tidal volume, MV: Minute ventilation, $ETCO_2$: End-tidal CO_2. Time capnography parameters: $S2_T$: phase 2 slope, $S3_T$: phase 3 slope. Volumetric capnography parameters: $S2_V$: phase 2 slope, $S3_V$: phase 3 slope, VDF: Fowler (anatomical) dead space, VDB: Bohr (physiological) dead space, VCO_2: Volume of exhaled CO_2 per breath. $*$: $p < 0.05$ vs. medium within mainstream or sidestream; $\#$: $p < 0.05$ vs. low within mainstream or sidestream; $\$$: $p < 0.05$ mainstream vs. sidestream within a condition.

Figure 3 shows the correlations between normalized shape factors, ventilation dead space parameters, and $ETCO_2$ measured using both main- and sidestream capnography across various breathing frequencies. Significant correlations were found for all capnographic parameters assessed by main- and sidestream techniques at all breathing rates. When comparing correlation coefficients, an increase in breathing rate significantly weakened the association for $Sn3_T$ ($p < 0.05$), while the correlation for VnDF showed a significant increase ($p < 0.05$).

We assessed the impact of altering breathing frequency as an intervention on capnogram indices, focusing on the relative differences when assessed by main- and sidestream capnography, as shown in Fig. 3. Significant correlations were observed for the relative changes in all capnogram parameters across various breathing frequencies. Furthermore, the analysis indicated that a higher breathing rate significantly enhanced the correlation for changes in Sn2T ($p < 0.05$) and reduced the correlation coefficients for changes in VnDB ($p < 0.05$).

The results of the Bland–Altman analyses are presented in Figs. S2-S4 (*online data supplement*), and a summary of the mean bias and limits of agreement are summarized in Table 3. Main- and sidestream capnography techniques demonstrated good agreement with a narrow bias for $ETCO_2$, VDB, and VnDB across all breathing rates. However, such analyses of other capnography shape factors and dead space parameters revealed systematic bias and wider limits of agreement when measured with both sidestream and mainstream techniques. Breathing frequency had significant effect on the agreement between the two techniques for all parameters ($p < 0.05$), except $Sn2_T$ and VDF. The absolute values of the measured parameters had significant effect on the differences between sidestream and mainstream techniques resulting in a proportional error (trend) for all parameters ($p < 0.05$), except $S3_T$ and VDB.

Discussion

The results of the present study demonstrate significant correlations between shape factor and ventilation dead space parameters obtained by mainstream and sidestream capnography in subjects breathing spontaneously. The respiratory rate significantly impacted all capnography parameters, regardless of the measurement technique used. However, both mainstream and sidestream approaches exhibited comparable abilities in detecting changes in capnography indices in response to variations of the breathing rate, as indicated by the excellent concordance between the two techniques. Conversely, the agreement between mainstream and sidestream measurements depends on the breathing frequency, exhibiting a broad range of variability from relatively poor for most outcomes to relatively close for $ETCO_2$ and physiological dead space.

The influence of breathing frequency on the amount of expired CO_2 with a particular focus on the $ETCO_2$ and V_T alterations is well documented[26,27]. While these changes are expected to manifest in alterations of capnogram shape factors and dead space parameters, there is a notable research gap in this respect. Increased breathing frequency results in steeper phase 2 and 3 slopes in the time domain, attributable to higher expiratory flows (Table 2, Fig. 2). This faster breathing reduces the gas transition zone between the conducting and respiratory zones, leading to a decrease in the $S2_V$. Anatomical and physiological dead space fractions demonstrate a positive relationship with breathing frequency, indicating less efficient gas exchange at higher rates. Although the overall changes are consistent across measurement techniques, significant discrepancies exist between side- and mainstream measurements for all capnogram parameters except for VDB. This discrepancy can be attributed to the fundamental difference between the two techniques. Sidestream estimates are biased by the axial gas diffusion in the sampling tube[3,19,20], which affects the dynamic response of the measurement system in a frequency-dependent manner.
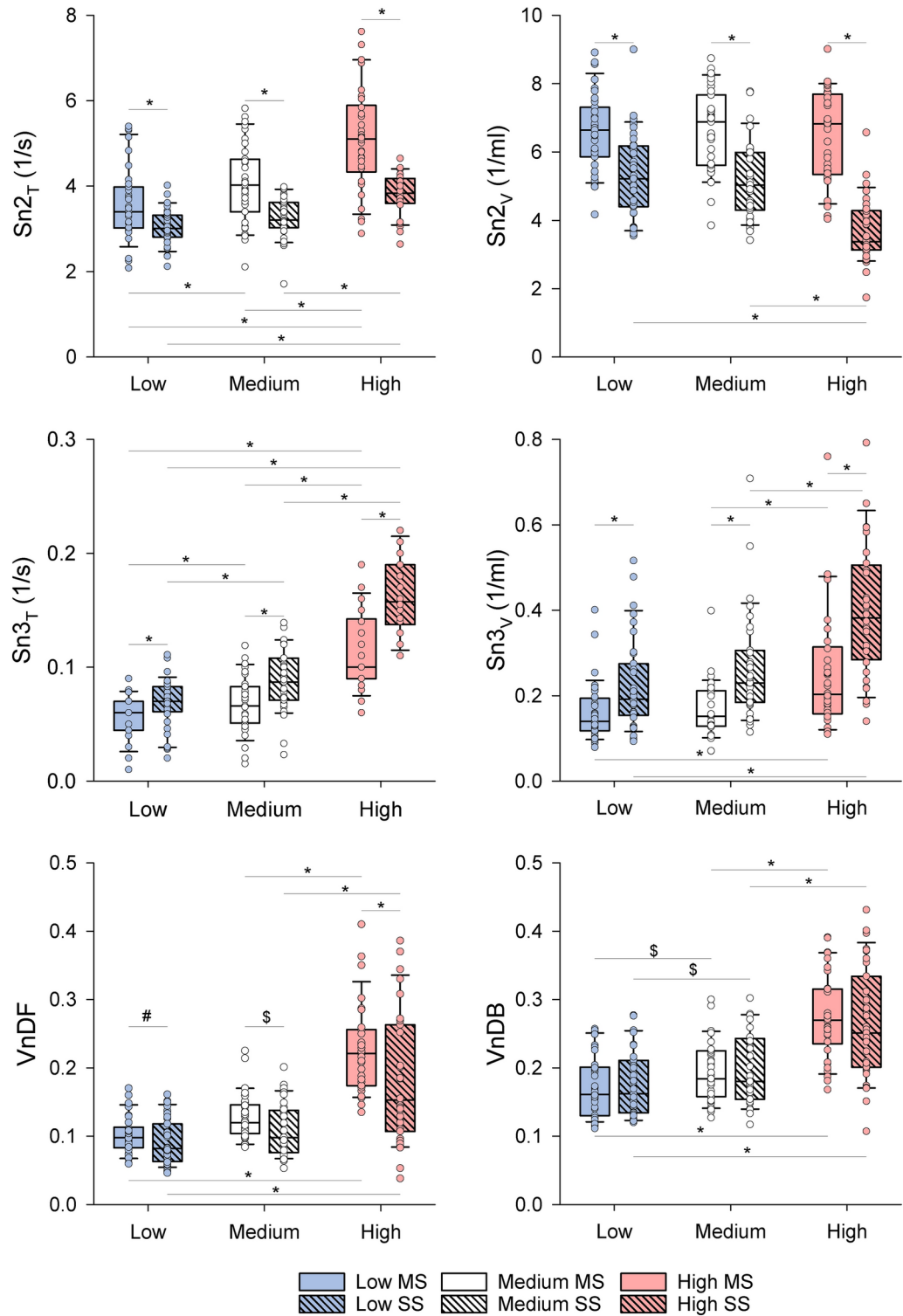
Fig. 2. Normalized phase 2 and 3 slopes obtained from time ($Sn2_T$, $Sn3_T$) and volumetric capnograms ($Sn2_V$, $Sn3_V$), Fowler's anatomical (VnDF) and Bohr's physiological (VnDB) dead space fractions measured with both mainstream (empty boxes) and sidestream (hatched boxes) techniques in spontaneously breathing subjects (n = 35) at low (blue), medium (white) and high (red) breathing frequencies. #: $p < 0.05$, \$: $p < 0.01$, *: $p < 0.001$.

The frequency-dependent discrepancy between the capnography parameters obtained by main- and sidestream techniques was further explored by analyzing their relationships. These analyzes generally revealed significant correlations between the shape factors and dead space indices with a wide range in the strength of associations (Fig. 3). Parameters related to the late phase of the expiration (phase 3 slopes and physiological dead space) exhibited very strong correlations since this part of the capnogram is less sensitive to the dynamic
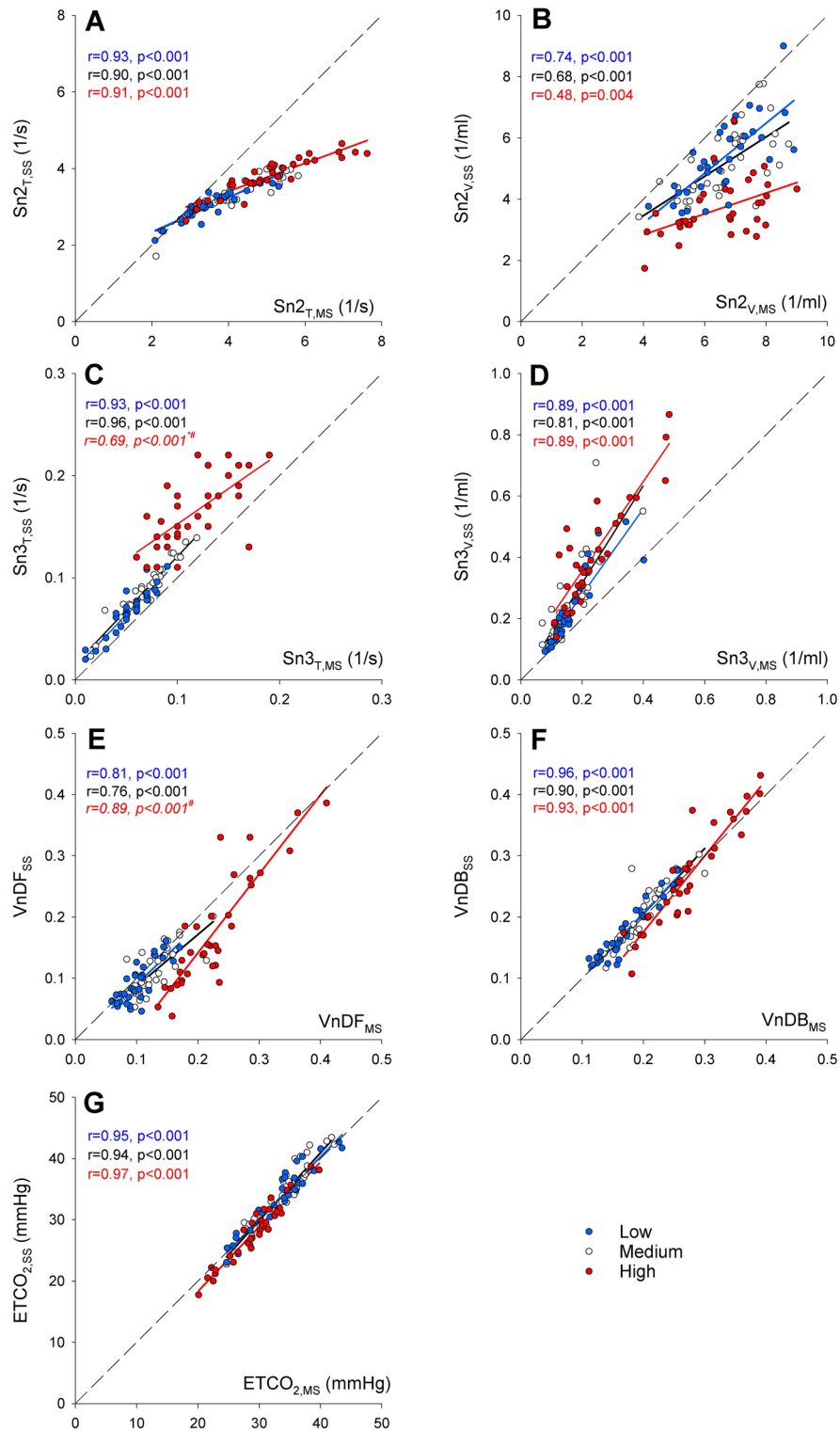
Fig. 3. Correlations between the absolute values of time and volumetric capnography indices measured by mainstream (MS, horizontal axis) and sidestream capnography (SS, vertical axis). Linear regressions for low (blue), medium (black) and high (red) breathing frequencies are shown as continuous lines, grey dashed lines indicate the lines of identity. Pearson correlation coefficients (r) and p values for each breathing rate are shown separately in each panel with the corresponding colors. *: r values $p < 0.05$ vs. low, #: r values $p < 0.05$ vs. medium. $ETCO_2$: end-tidal CO_2; $Sn2_T$ and $Sn3_T$: normalized phase 2 and 3 slopes in time capnogram, respectively; $Sn2_V$ and $Sn3_V$: normalized phase 2 and 3 slopes in volumetric capnogram, respectively; VnDF: Fowler (anatomical) dead space fraction; VnDB: Bohr (physiological) dead space fraction.

	Breathing frequency	Mean bias (%)	95% Limits of agreement (%)		Proportional error
ETCO$_2$	Low*	−0.2 (−1.9 – 1.5)	−9.8 (−11.0 – −9.0)	9.4 (8.5 – 10.1)	−0.003$^\$$ (−0.005 – −0.002)
	Normal #	−0.8 (−2.5 – 1.0)	−10.8 (−11.6 – −9.9)	9.2 (8.3 – 10.0)	
	High §	4.4 (2.7 – 6.0)	−5.1 (−6.0 – −4.3)	13.9 (13.1 – 14.5)	
S2$_T$	Low#	13.9 (9.8 – 18.1)	−9.7 (−12.0 – −8.0)	37.5 (35.4 – 39.6)	0.003$^\$$ (0.002 – 0.005)
	Normal#	18.5 (13.9 – 23.1)	−7.7 (−10.0 – −5.4)	44.7 (42.4 – 47.0)	
	High§*	31.5 (26.7 – 36.3)	4.6 (2.2 – 7.1)	58.4 (56.0 – 60.9)	
Sn2$_T$	Low	14.1 (10.2 – 18.1)	−8.4 (−10.0 – −6.0)	36.7 (34.7 – 38.7)	0.129$^\$$ (0.111 – 0.147)
	Normal	19.3 (15.5 – 23.1)	−2.5 (−4.4 – −0.0)	41.1 (39.2 – 43.0)	
	High	27.1 (22.7 – 31.5)	2.5 (0.3 – 4.8)	51.7 (49.5 – 53.9)	
S3$_T$	Low*#	−23.2 (−28.3 – −18.1)	−52.2 (−55.0 – −50.0)	5.9 (3.3 – 8.4)	0.031 (−0.010 – 0.073)
	Normal§	−27.4 (−32.6 – −22.1)	−57.4 (−60.1 – −54.8)	2.7 (0.0 – 5.4)	
	High§	−32.4 (−40.0 – −24.7)	−75.4 (−79.4 – −71.5)	10.7 (6.8 – 14.6)	
Sn3$_T$	Low*#	−23.0 (−27.8 – −18.1)	−50.6 (−53.0 – −48.0)	4.6 (2.2 – 7.1)	2.403$^\$$ (1.250 – 3.557)
	Normal§#	−26.6 (−31.3 – −22.0)	−53.3 (−55.7 – −51.0)	0.0 (−2.3 – 2.4)	
	High§*	−36.8 (−44.0 – −29.5)	−77.3 (−81.0 – −73.6)	3.8 (−0.1 – 7.5)	
S2$_V$	Low#	21.9 (16.9 – 26.9)	−6.5 (−9.0 – −4.0)	50.3 (47.8 – 52.8)	−0.001$^\$$ (−0.002 – −0.001)
	Normal#	24.7 (18.8 – 30.6)	−9.1 (−12.1 – −6.2)	58.5 (55.5 – 61.5)	
	High§*	59.4 (52.4 – 66.2)	20.5 (17.0 – 24.0)	98.2 (94.7 – 101.7)	
Sn2$_V$	Low#	22.1 (17.1 – 27.2)	−6.7 (−9.0 – −4.0)	50.9 (48.4 – 53.4)	−0.061$^\$$ (−0.094 – −0.028)
	Normal#	25.5 (20.0 – 30.8)	−5.3 (−8.0 – −2.6)	56.2 (53.5 – 58.9)	
	High§*	55.2 (48.0 – 62.2)	15.3 (11.6 – 18.9)	95.1 (91.5 – 98.7)	
S3$_V$	Low*#	−29.8 (−35.2 – −24.2)	−61.1 (−64.0 – −58.0)	1.6 (−1.0 – 4.3)	−0.015$^\$$ (-0.025 – -0.005)
	Normal§	−42.3 (−50.3 – −34.3)	−87.7 (−91.7 – −83.7)	3.1 (−0.9 – 7.1)	
	High§	−48.5 (−56.6 – −40.3)	−92.5 (−96.8 – −88.3)	−4.4 (−8.7 – −0.1)	
Sn3$_V$	Low*#	−29.6 (−34.8 – −24.3)	−59.5 (−62.0 – −57.0)	0.3 (−2.3 – 3.0)	−0.461$^\$$ (−0.850 – −0.071)
	Normal§	−41.6 (−49.1 – −31.2)	−84.3 (−88.1 – −80.6)	1.1 (−2.7 – 4.8)	
	High §	−52.7 (−60.1 – −45.4)	−92.6 (−96.4 – −88.7)	−12.8 (−16.7 – −9.1)	
VDF	Low	14.5 (4.4 – 24.7)	−43.6 (−48.7 – −38.4)	72.6 (67.5 – 77.7)	0.005$^\$$ (0.003 – 0.006)
	Normal	19.3 (12.4 – 26.1)	−19.9 (−23.4 – −16.4)	58.5 (55.0 – 61.9)	
	High	37.5 (25.8 – 49.1)	−29.0 (−34.9 – −23.1)	104.0 (98.1 – 109.9)	
VnDF	Low#	15.9 (5.7 – 26.0)	−41.1 (−46.3 – −35.9)	72.8 (67.6 – 78.0)	−2.517$^\$$ (−3.400 – −1.633)
	Normal#	16.8 (9.1 – 24.4)	−27.0 (−30.9 – −23.2)	60.6 (56.7 – 64.4)	
	High§*	34.3 (23.1 – 45.5)	−28.8 (−34.4 – −23.0)	97.3 (91.6 – 103.0)	
VDB	Low*#	−2.6 (−6.0 – 8.5)	−22.1 (−23.8 – −20.4)	17.0 (15.2 – 18.7)	0.000 (0.000 – 0.000)
	Normal§#	1.0 (−2.1 – 4.1)	−16.8 (−18.4 – −15.3)	18.8 (17.3 – 20.4)	
	High§*	11.7 (4.0 – 19.3)	−32.0 (−35.8 – −28.1)	55.3 (51.5 – 59.1)	
VnDB	Low*#	−1.8 (−4.9 – 1.3)	−19.2 (−20.8 – −17.6)	15.6 (14.1 – 17.2)	−0.769$^\$$ (−1.173 – −0.364)
	Normal§#	−1.5 (−5.3 – 2.2)	−23.1 (−25.0 – −21.2)	20.0 (18.1 – 21.9)	
	High§*	4.7 (−0.2 – 9.7)	−23.2 (−25.8 – −20.7)	32.7 (30.1 – 35.1)	

Table 3. Mean bias and 95% limits of agreement are determined by Bland–Altman analyses in spontaneously breathing healthy subjects (n = 35). 95% confidence intervals are presented in parentheses. Trends in the data are presented as proportional error with 95% confidence intervals in parentheses. ETCO$_2$: end-tidal CO$_2$. Time capnography parameters: S2$_T$: phase 2 slope, Sn2$_T$: normalized phase 2 slope (S2T/ETCO$_2$), S3$_T$: phase 3 slope, Sn3$_T$: normalized phase 3 slope (S3$_T$/ETCO$_2$). Volumetric capnography parameters: S2$_V$: phase 2 slope, Sn2$_V$: normalized phase 2 slope (S2$_V$/ETCO$_2$), S3$_V$: phase 3 slope, Sn3$_V$: normalized phase 3 slope (S3$_V$/ETCO$_2$), VDF: Fowler (anatomical) dead space, VnDF: normalized Fowler (anatomical) dead space (VnDF/VT), VDB: Bohr (physiological) dead space, VnDB: normalized Bohr (physiological) dead space (VnDB/VT). Significant effects of breathing frequency are presented with symbols: *: $p < 0.05$ versus normal; #: $p < 0.05$ versus high; §: $p < 0.05$ versus low. $^\$$: $p < 0.05$ versus zero in the proportional error.

distortion caused by the sampling tube. Conversely, distal gas analysis by sidestream approach is more prone to a bias for the parameters associated with the early phase of expiration (phase 2 slopes and anatomical dead space), where the dynamic changes in the volume and pressure are dominant. Interestingly, while alteration in the breathing rate affected the absolute values of the capnogram parameters, this intervention had a significant effect on the strength of correlation only for Sn3$_T$. This finding indicates that sidestream assessments of the capnogram indices reflect those measured by the mainstream technique as a reference, except for the phase 3

slope time domain at high breathing rate. This uncertainty in the sidestream assessment can be attributed to the shortened breathing cycle, which blurs the transitions between the phases (Fig. S1), thereby diminishing the reliability of the sidestream estimates.

We also extended the analysis to compare the agreement between main- and sidestream capnography parameters (Table 3 and Figures S2-S4). These analyses revealed good agreements for $ETCO_2$ and physiological dead space measurements (VDB and VnDB). However, the agreements for other capnogram parameters were relatively poor, characterized by large biases, wide limits of agreement, and significant proportional errors. As expected, increasing breathing frequency weakened the agreements due to the impaired dynamic response of the sidestream estimates. While the devices are not interchangeable for assessing the absolute values of the capnogram parameters, a good concordance was observed in the changes of these indices to alterations in breathing rate as a challenge (Fig. 4). This finding suggests that both capnography techniques can effectively serve as trend monitors for detecting changes in ventilation and/or ventilation-perfusion matching.

The strength of correlation and the limits of agreement in S3T and S3V are comparable to those obtained earlier in mechanically ventilated patients[20]. However, the concordance between the main- and sidestream estimates for phase 2 slopes and dead space fractions in subjects breathing spontaneously is markedly stronger than the correlations and agreements observed under mechanical ventilation[20]. This finding is of particular interest, given that mechanical ventilation theoretically provides strictly monotonous and uniformly controlled pressure and flow conditions in the lungs, in contrast to the variability seen with spontaneous breathing. The stronger association observed between the main- and sidestream techniques may be attributed to the fundamentally different pressure conditions experienced during spontaneous breathing compared to mechanical ventilation. Alternating positive airway pressure during mechanical ventilation introduces significant dynamic variations in sampling flow rate, which distorts the sidestream capnogram, especially in the rapidly changing phases (i.e. phase 2)[28]. During spontaneous breathing, however, the amplitude of negative pressure swings at the inlet is physiologically smaller. Thus, sidestream measurements exhibit less bias from the pressure fluctuations that occur during transitions between the inspiratory and expiratory phases of spontaneous breathing.

Some methodological aspects and limitations warrant consideration. While consistent changes in the capnogram parameters were evidenced across different breathing frequencies, our study did not aim to induce major gas exchange disturbances through these voluntary changes in breathing rate. Therefore, we limited the selection of breathing rates to those within physiological ranges to ensure that gas exchange parameters remain in the physiological range. The use of controlled breathing rates can also pose some limitations; however allowing spontaneous breathing frequencies would have introduced additional variabilities and would have complicated the comparison. Another important aspect of our study is the inclusion of a somewhat heterogeneous population, including a few patients with mild cardiorespiratory disorders, thereby supporting the generalizability of our findings to a wider population. Furthermore, despite the study being conducted with a moderate number of patients, the statistical tests achieved high power levels. This ensures that we can draw statistical conclusions with a high degree of confidence.

In summary, we simultaneously measured shape factor parameters and ventilation dead space fractions in spontaneously breathing subjects using both main- and sidestream capnography. Our analysis revealed consistent assessments of $ETCO_2$ and Bohr physiological dead space across measurement techniques, indicating these assessments are technique-invariant. In contrast, other capnography indices varied depending on the expired gas analysis site. Despite a general lack of agreement across different measurements, our study found strong and significant correlations in the absolute values of capnography indices, particularly in their ability to reflect relative changes associated with altered breathing rates. Given the consideration of mainstream capnography as the reference technique, the observed close association underscores the effectiveness of sidestream capnography in monitoring within-subject variations in shape factors and dead space fractions. Consequently, sidestream capnography emerges as a reliable method for monitoring trends both in the time and volumetric domain in clinical scenarios where mainstream technique is not available or not feasible (e.g., polysomnography or noninvasive ventilation), allowing the assessment of alterations in lung ventilation, and evaluating ventilation-perfusion matching in spontaneously breathing subjects.
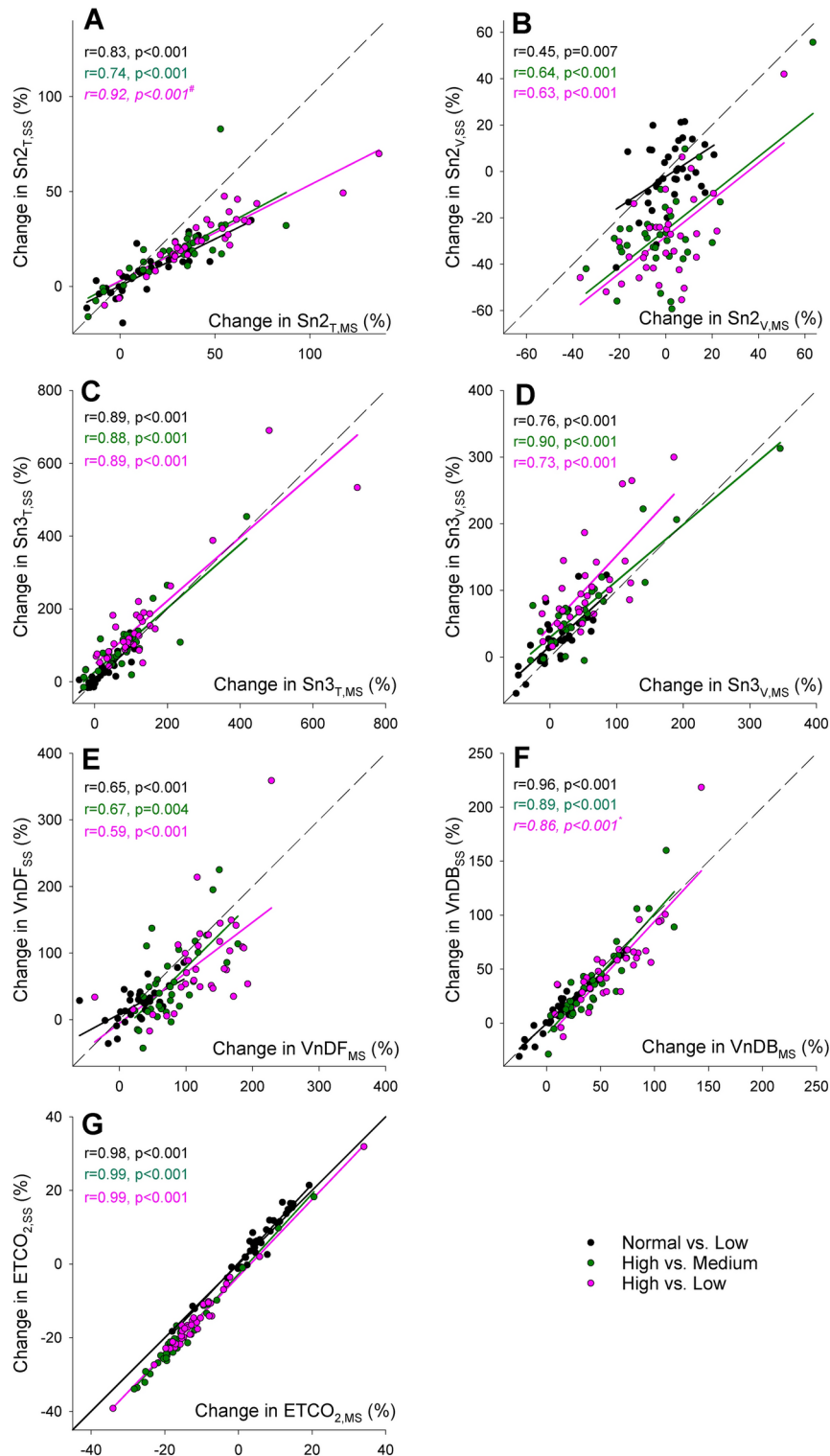
Fig. 4. Correlations between the changes in time and volumetric capnography indices to alterations of breathing frequency measured by mainstream (MS, horizontal axis) and sidestream capnography (SS, vertical axis). Linear regressions for the transitions from medium to low (black), high to medium (green) and high to low (magenta) breathing frequencies are shown as continuous lines, grey dashed lines indicate the lines of identity. Pearson correlation coefficients (r) and p values for each change in breathing rate are shown separately in each panel with the corresponding colors. *: r values $p < 0.05$ versus normal to low, #: r values $p < 0.05$ versus high to medium. $ETCO_2$: end-tidal CO_2; $Sn2_T$ and $Sn3_T$: normalized phase 2 and 3 slopes in time capnogram, respectively; $Sn2_V$ and $Sn3_V$: normalized phase 2 and 3 slopes in volumetric capnogram, respectively; VnDF: Fowler (anatomical) dead space fraction; VnDB: Bohr (physiological) dead space fraction.

Data availability

The datasets used and/or analyzed during the current study are available from the corresponding author on reasonable request.

References

1. Ortega, R., Connor, C., Kim, S., Djang, R. & Patel, K. Monitoring ventilation with capnography. *N Engl. J. Med.* **367**, e27 (2012).
2. Walsh, B. K., Crotwell, D. N. & Restrepo, R. D. Capnography/Capnometry during mechanical ventilation: 2011. *Respir. Care* **56**, 503–509 (2011).
3. Thompson, J. E. & Jaffe, M. B. Capnographic waveforms in the mechanically ventilated patient. *Respir. Care* **50**, 100–108 (2005).
4. Owens, B. & Hall, C. Application of end-tidal CO_2 monitoring to ICU management. *Crit. Care Nurs. Q* **47**, 157–162 (2024).
5. Kremeier, P., Bohm, S. H. & Tusman, G. Clinical use of volumetric capnography in mechanically ventilated patients. *J. Clin. Monit. Comput.* **34**, 7–16 (2020).
6. Csorba, Z. et al. Capnographic parameters in ventilated patients: correspondence with airway and lung tissue mechanics. *Anesth. Analg.* **122**, 1412–1420 (2016).
7. Howe, T. A., Jaalam, K., Ahmad, R. & Sheng, C. K. Nik Ab Rahman NH: The use of end-tidal capnography to monitor non-intubated patients presenting with acute exacerbation of asthma in the emergency department. *J. Emerg. Med.* **41**, 581–589 (2011).
8. Nik Hisamuddin, N. A. et al. Correlations between capnographic waveforms and peak flow meter measurement in emergency department management of asthma. *Int. J. Emerg. Med.* **2**, 83–89 (2009).
9. Delerme, S. et al. Concordance between capnography and capnia in adults admitted for acute dyspnea in an ED. *Am. J. Emerg. Med.* **28**(6), 711–714. https://doi.org/10.1016/j.ajem.2009.04.028 (2010).
10. Scully, K. R., Rickerby, J. & Dunn, J. Implementation science: incorporating obstructive sleep apnea screening and capnography into everyday practice. *J. Perianesth. Nurs.* **35**, 7–16 (2020).
11. Kim, S. M. et al. Capnography for assessing nocturnal hypoventilation and predicting compliance with subsequent noninvasive ventilation in patients with ALS. *PLoS ONE* **6**, e17893 (2011).
12. Magnan, A. et al. End-tidal CO_2 analysis in sleep apnea syndrome. Conditions for use. *Chest* **103**, 129–131 (1993).
13. Damam, S. et al. Navigating pediatric capnography: a comprehensive review of scope and limitations. *Cureus* **16**, e53289 (2024).
14. Eipe, N. & Doherty, D. R. A review of pediatric capnography. *J. Clin. Monit. Comput.* **24**, 261–268 (2010).
15. Bullock, A., Dodington, J. M., Donoghue, A. J. & Langhan, M. L. Capnography use during intubation and cardiopulmonary resuscitation in the pediatric emergency department. *Pediatr. Emerg. Care* **33**, 457–461 (2017).
16. Blanch, L., Romero, P. V. & Lucangelo, U. Volumetric capnography in the mechanically ventilated patient. *Minerva Anestesiol.* **72**, 577–585 (2006).
17. Breen, P. H., Mazumdar, B. & Skinner, S. C. Capnometer transport delay: measurement and clinical implications. *Anesth. Analg.* **78**, 584–586 (1994).
18. Brunner, J. X. & Westenskow, D. R. How the rise time of carbon dioxide analysers influences the accuracy of carbon dioxide measurements. *Br. J. Anaesth.* **61**, 628–638 (1988).
19. Anderson, C. T. & Breen, P. H. Carbon dioxide kinetics and capnography during critical care. *Crit. Care* **4**, 207–215 (2000).
20. Balogh, A. L. et al. Capnogram slope and ventilation dead space parameters: comparison of mainstream and sidestream techniques. *Br. J. Anaesth.* **117**, 109–117 (2016).
21. Tusman, G., Scandurra, A., Bohm, S. H., Suarez-Sipmann, F. & Clara, F. Model fitting of volumetric capnograms improves calculations of airway dead space and slope of phase III. *J. Clin. Monit. Comput.* **23**, 197–206 (2009).
22. Tolnai, J. et al. Changes in lung mechanics and ventilation-perfusion match: comparison of pulmonary air- and thromboembolism in rats. *BMC Pulm Med.* **24**, 27 (2024).
23. Fowler, W. S. Lung function studies; the respiratory dead space. *Am. J. Physiol.* **154**, 405–416 (1948).
24. Bohr C: **Über die Lungenatmung.** *Skan Arch Physiol* 1891**:**236–238.
25. Bland, J. M. & Altman, D. G. Statistical methods for assessing agreement between two methods of clinical measurement. *Lancet* **1**, 307–310 (1986).
26. Mehta, J. H., Williams, G. W. 2nd., Harvey, B. C., Grewal, N. K. & George, E. E. The relationship between minute ventilation and end tidal CO_2 in intubated and spontaneously breathing patients undergoing procedural sedation. *PLoS ONE* **12**, e0180187 (2017).
27. West JB, Luks A: *West's respiratory physiology : the essentials.* Tenth edition. edn. Philadelphia: Wolters Kluwer; 2016.
28. Farmery, A. D. & Hahn, C. E. A method of reconstruction of clinical gas-analyzer signals corrupted by positive-pressure ventilation. *J. Appl. Physiol.* **2001**(90), 1282–1290 (1985).

Author contributions

J.T., G.H.F., Z.N, and F.P. conceived and designed the research; J.T., G.H.F., I.T., and F.P. performed the experiments; J.T., G.H.F., F.R., and F.P. analyzed the data; J.T., G.H.F., B.B., Z.N., and F.P. interpreted the results of the experiments; J.T., G.H.F., and F.P. prepared the figures and tables; J.T., G.H.F., and F.P. drafted the manuscript; J.T., F.R, I.T., B.B., Z.N., G.H.F., and F.P. edited and revised the manuscript; all authors approved the final version of the manuscript.

Funding

Declarations

Competing interests

The authors declare no competing interests.

Ethical approval and consent to participate

Regional and Institutional Review Board of Human Investigations of the University of Szeged, Hungary (No. 186/2020; address: 6720 Szeged, Dugonics tér 13. Hungary, 25 January 2021).

Consent for publication

Not applicable.

Additional information

Supplementary Information The online version contains supplementary material available at https://doi.org/10.1038/s41598-024-75808-0.

Correspondence and requests for materials should be addressed to F.P.

Reprints and permissions information is available at www.nature.com/reprints.

Publisher's note Springer Nature remains neutral with regard to jurisdictional claims in published maps and institutional affiliations.